

## MASSIVE STARS AND THEIR ENVIRONMENT: LIGHT AND SHADOWS

Tim Freyer and Gerhard Hensler

Institut für Theoretische Physik und Astrophysik der Universität Kiel, Germany

### RESUMEN

Estudiamos, con un código 2D de hidrodinámica radiativa, la interacción de una estrella de  $60 M_{\odot}$  con el medio interestelar circundante. En algunos momentos de la evolución la región H II interacciona fuertemente con la burbuja formada por el viento estelar, requiriendo la inclusión de la radiación ionizante y el viento estelar para describir apropiadamente al medio circunestelar. Se forman un amplia variedad de estructuras interesantes como nubes, cascarones y dedos. También presentamos la evolución temporal de la ionización y la energía cinética del gas interestelar.

### ABSTRACT

We study the interaction of a  $60 M_{\odot}$  star with its surrounding interstellar medium numerically using a 2D radiation hydrodynamics code. It turns out that for certain stages of evolution the H II region strongly interacts with the wind-blown bubble, requiring the consideration of both, the ionizing radiation and the stellar wind for an appropriate description of the circumstellar medium. A variety of interesting structures like clouds, shells, and fingers can be found. We also present quantitative results for the transformation of the stellar input energy into kinetic energy of the interstellar medium and its ionization as a function of time.

*Key Words:* **H II REGIONS — HYDRODYNAMICS — INSTABILITIES — ISM: BUBBLES — ISM: STRUCTURE**

### 1. INTRODUCTION

Massive stars have an enormous impact on the energy budget of the interstellar medium (ISM). Their radiation field ionizes the circumstellar gas and produces an H II region that expands into the neutral ambient medium (Yorke 1986; Franco et al. 1998). The fast stellar wind creates shocks that form a so called wind-blown bubble (WBB) which evolves into the H II region (Castor, McCray, & Weaver 1975; Weaver et al. 1977; Mac Low these proceedings). Though the classical picture of WBBs around main sequence stars is supported by the discovery of shells around O-type stars (Oey & Massey 1994; Marston 1995; Cappa & Benaglia 1998), there is no observational indication yet for hot gas in these bubbles (see the papers by Chu and Mac Low in these proceedings).

Numerical simulations (Różyczka 1985; García-Segura, Mac Low, & Langer 1996; Strickland & Stevens 1998) have become a powerful tool to study the evolution of WBBs with respect to the effects that cannot yet be described within an analytical framework. We perform 2D radiation-hydrodynamic calculations of the interaction between an isolated massive star and its surrounding ISM. The model presented in this paper considers the hydrodynamic evolution of the gas around a star with an initial mass of  $60 M_{\odot}$  coupled with radiation transfer, time dependent ionization of hydrogen, and a realistic description of cooling. The goals of these model calculations are to examine the combined influence of both wind and ionizing radiation on the dynamical evolution of circumstellar matter around massive stars and to improve our knowledge of the energy transfer from stars to the ISM in galaxies (Lasker 1967; Abbott 1982).

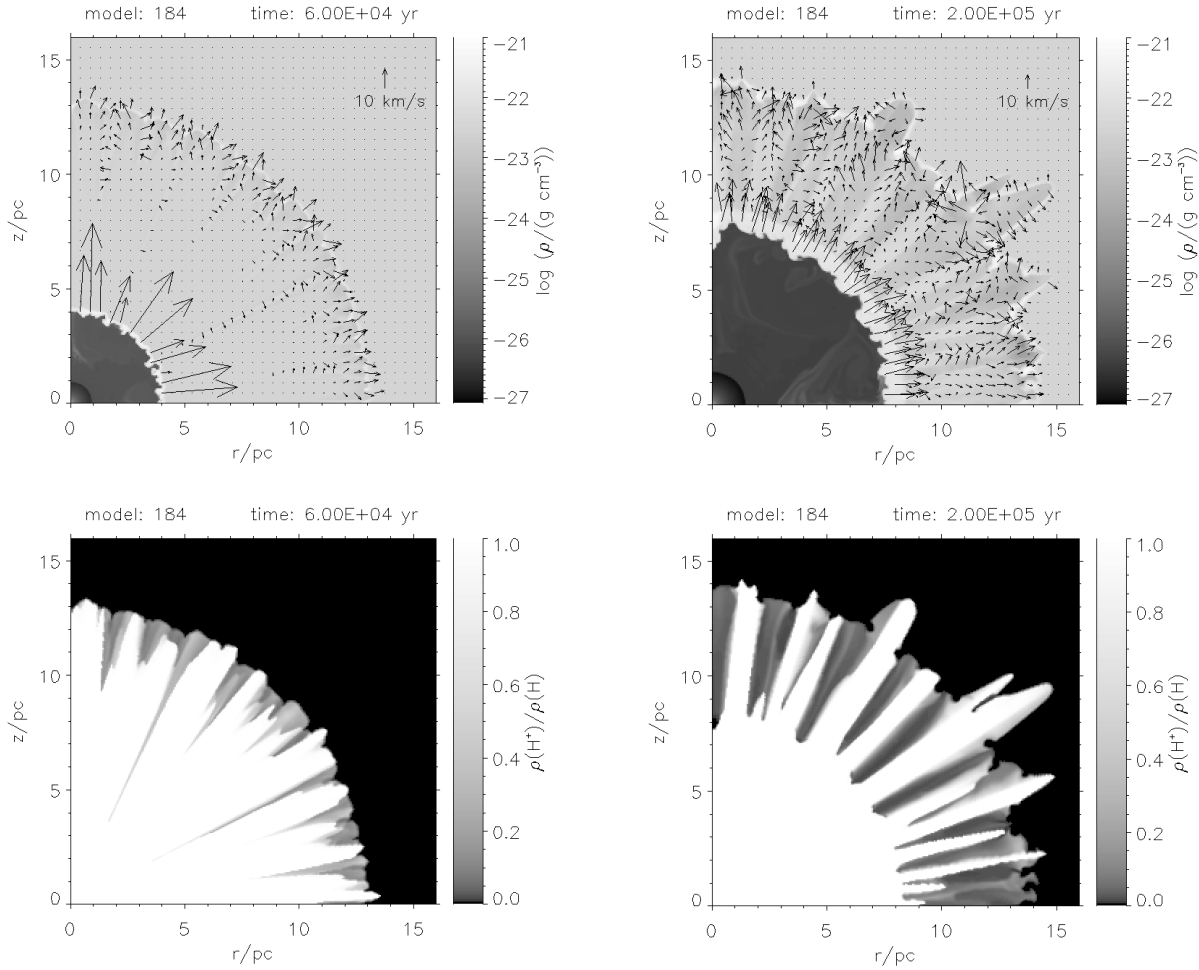


Fig. 1. Circumstellar density (upper panels) and degree of H-ionization (lower panels) for the model described in this paper at the age of 60,000 yr (left panels) and  $2 \times 10^5$  yr (right panels). The star is located in the center of the coordinate system. Velocity arrows are overlaid on the density plots. Arrows in the free-flowing wind and in the hot bubble have been omitted for clarity.

## 2. NUMERICAL METHODS

The basic numerical methods and the results of test calculations have already been described in Yorke & Kaisig (1995) and Yorke & Welz (1996). Here, we only give a very short summary of the code's properties. The hydrodynamical equations are solved numerically in one quadrant of a cylindrical Eulerian grid. The code uses a second order finite-differencing scheme and von Neumann-Richtmyer artificial viscosity for the treatment of shocks. Multiply nested grids are inserted to enhance the resolution near the star. The hydrogen ionization structure is determined in every time step. The absorption of the stellar Lyman continuum is calculated along radial lines of sight. Instead of "flux-limited diffusion" we used the "on-the-spot" approximation for the treatment of the diffuse radiation field to save CPU-time. The only heating process considered is the photoionization of hydrogen. The treatment of cooling depends on the temperature of the gas. For temperatures below 15,000 K the most important cooling processes are explicitly calculated. These are: bremsstrahlung, collisionally excited H-Ly $\alpha$  emission, collisional ionization of hydrogen, and the most important cooling lines of [O II], [O III], and [N II] (with an assumption about nitrogen and oxygen ionization from the degree of hydrogen ionization). For temperatures above  $10^5$  K the interstellar cooling function from Sarazin & White (1987) is used

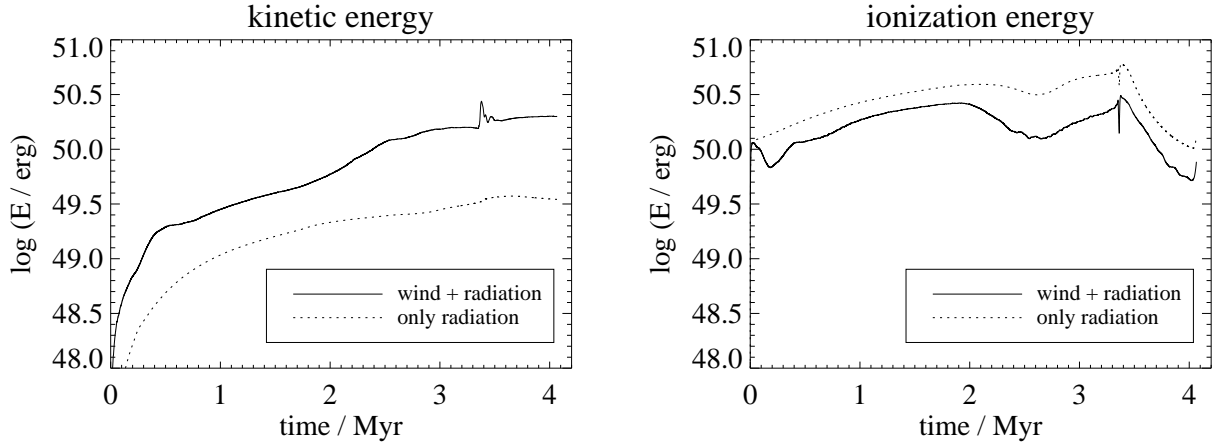


Fig. 2. Kinetic energy of circumstellar gas motion (left panel) and ionization energy (13.6 eV per ionized hydrogen atom, right panel) for our model during the whole life of the  $60 M_{\odot}$  star (with and without wind) until it explodes as a supernova.

(including the correction stated by Soker 1990). This cooling function is based on the assumption of collisional ionization equilibrium. In the temperature range between 15,000 K and  $10^5$  K we interpolate between both values. Dust is not considered for the models presented here.

We employed two different resolutions in our calculations. The high resolution model shown in Figure 1 has a resolution of 0.25 pc per cell on the coarsest grid that covers  $(64 \text{ pc})^2$ . 6 grids are nested into the coarsest grid, so that the resolution close to the star is enhanced by a factor  $2^6 = 64$  in each dimension. The calculation used to produce the data in Figure 2 has four times lower resolution (in each dimension). We start the calculations with an initially undisturbed, homogeneous background ISM with  $T = 200$  K and  $n_{\text{H}} = 20 \text{ cm}^{-3}$  (as in García-Segura et al. 1996). The stellar parameters (mass-loss rate, terminal velocity of the wind, effective temperature and luminosity), which are used as time dependent boundary conditions in our calculations, are also taken from García-Segura et al. (1996).

### 3. RESULTS AND DISCUSSION

Figure 1 shows density, degree of H-ionization, and velocity structure of our  $60 M_{\odot}$  model. At the very beginning of the evolution the photoionized H II region and the WBB evolve independently of each other. After the shell of the WBB had collapsed to a thin shell, it became subject to the thin-shell instability (Vishniac 1983; Ryu & Vishniac 1988; Vishniac & Ryu 1989) that amplified density fluctuations from the numerical noise and produced some density knots in the shell. The optical depth for Lyman continuum photons is enhanced along radial lines of sight through density knots, while it is lowered for other lines of sight. In other words: the density knots in the WBB shell cast shadows into the H II region so that the gas behind the density knots starts to recombine, while the H II region is extended along the lines of sight between the shadows because of the Lyman continuum photon excess there (ionized “fingers”). The situation is depicted in the left panels of Figure 1 at an age of 60,000 yr. It should be pointed out here that this deformation of the photoionization front is a consequence of the interaction of the WBB with the photoionized H II region and that it is not solely caused by the photoionization front instability described by García-Segura & Franco (1996). The deformation of the ionization front in our model is strongly triggered and amplified by the evolution of the WBB shell. The recombing gas in the shadowed regions loses pressure compared to the remaining part of the H II region. The resulting pressure gradients force a mass flux into the shadows. Density enhancements (neutral “spokes”) in the shadows appear, which further increase the optical depth along these lines of sight, while the density in the inter-shadow regions drops and the extension of the H II region along these lines of sight rises. The “spokes” are swept up by the WBB shell enhancing the density clumps there. This can be seen in the right panels of

Figure 1. This is an impressive example of how the interaction of the WBB with the photoionized H II region leads to the formation of a variety of morphological structures even from an initially homogeneous ambient density distribution. Nevertheless, the structure described above is only a transient phenomenon as the whole H II region becomes more and more swept up by the WBB shell.

In Figure 2 the kinetic energy of the circumstellar gas motion and the total ionization energy for this model are shown as a function of time until the star is supposed to explode as a supernova. One can see that the total ionization energy reaches approximately  $10^{50}$  erg very soon after the start of the calculation. The dynamical response of the circumstellar gas (the expansion of the H II region and the acceleration of the swept-up material by the WBB) takes much longer and can be seen in the gradual increase of the kinetic energy. For comparison, the same data is also plotted for the identical model which considers only the stellar radiation but neglects the stellar wind. Obviously, the total kinetic energy in the calculation that considers the wind is always higher than in the corresponding calculation without wind because the kinetic energy of the WBB shell is added to the kinetic energy of the expanding H II region. The situation is different for the total ionization energy. Though there is additional energy input by the stellar wind, the ionization energy is lower than in the calculation without wind by 0.2 to 0.5 dex for most of the time. Here the formation of dense structures in the H II region (shell, spokes) results in a higher cooling power of the gas. For details and further results see Freyer, Hensler, & Yorke (2000).

The authors would like to thank Harold Yorke, Don Cox, José Franco, and Mordecai-Mark Mac Low for a lot of helpful comments and stimulating discussions on this project over the past years. Financial support by the Deutsche Forschungsgemeinschaft (DFG) under grant number He 1487/17 is gratefully acknowledged. The computations were performed at the Rechenzentrum der Universität Kiel, the Konrad-Zuse-Zentrum für Informationstechnik in Berlin, and the John von Neumann-Institut für Computing in Jülich.

#### REFERENCES

- Abbott, D. C. 1982, *ApJ*, 263, 723  
 Cappa, C. E., & Benaglia, P. 1998, *AJ*, 116, 1906  
 Castor, J., McCray, R., & Weaver, R. 1975, *ApJ*, 200, L107  
 Franco, J., Díaz-Miller, R. I., Freyer, T., & García-Segura, G. 1998, in *ASP Conf. Ser. Vol. 141, Astrophysics from Antarctica*, ed. G. Novak & R. H. Landsberg (San Francisco: ASP), 154  
 Freyer, T., Hensler, G., & Yorke, H. W. 2000, in preparation  
 García-Segura, G., & Franco, J. 1996, *ApJ*, 469, 171  
 García-Segura, G., Mac Low, M.-M., & Langer, N. 1996, *A&A*, 305, 229  
 Lasker, B. M. 1967, *ApJ*, 149, 23  
 Marston, A. P. 1995, *AJ*, 109, 1839  
 Oey, M. S., & Massey, P. 1994, *ApJ*, 425, 635  
 Różyczka, M. 1985, *A&A*, 143, 59  
 Ryu, D., & Vishniac, E. T. 1988, *ApJ*, 331, 350  
 Sarazin, C. L., & White, R. E. 1987, *ApJ*, 320, 32  
 Soker, N. 1990, *AJ*, 99, 1869  
 Strickland, D. K., & Stevens, I. R. 1998, *MNRAS*, 297, 747  
 Vishniac, E. T. 1983, *ApJ*, 274, 152  
 Vishniac, E. T., & Ryu, D. 1989, *ApJ*, 337, 917  
 Weaver, R., McCray, R., Castor, J., Shapiro, P., & Moore, R. 1977, *ApJ*, 218, 377  
 Yorke, H. W. 1986, *ARAA*, 24, 49  
 Yorke, H. W., & Kaisig, M. 1995, *Comp. Phys. Comm.*, 89, 29  
 Yorke, H. W., & Welz, A. 1996, *A&A*, 315, 555

Tim Freyer and Gerhard Hensler: Institut für Theoretische Physik und Astrophysik der Universität Kiel, D-24098 Kiel, Germany (freyer, hensler@astrophysik.uni-kiel.de).